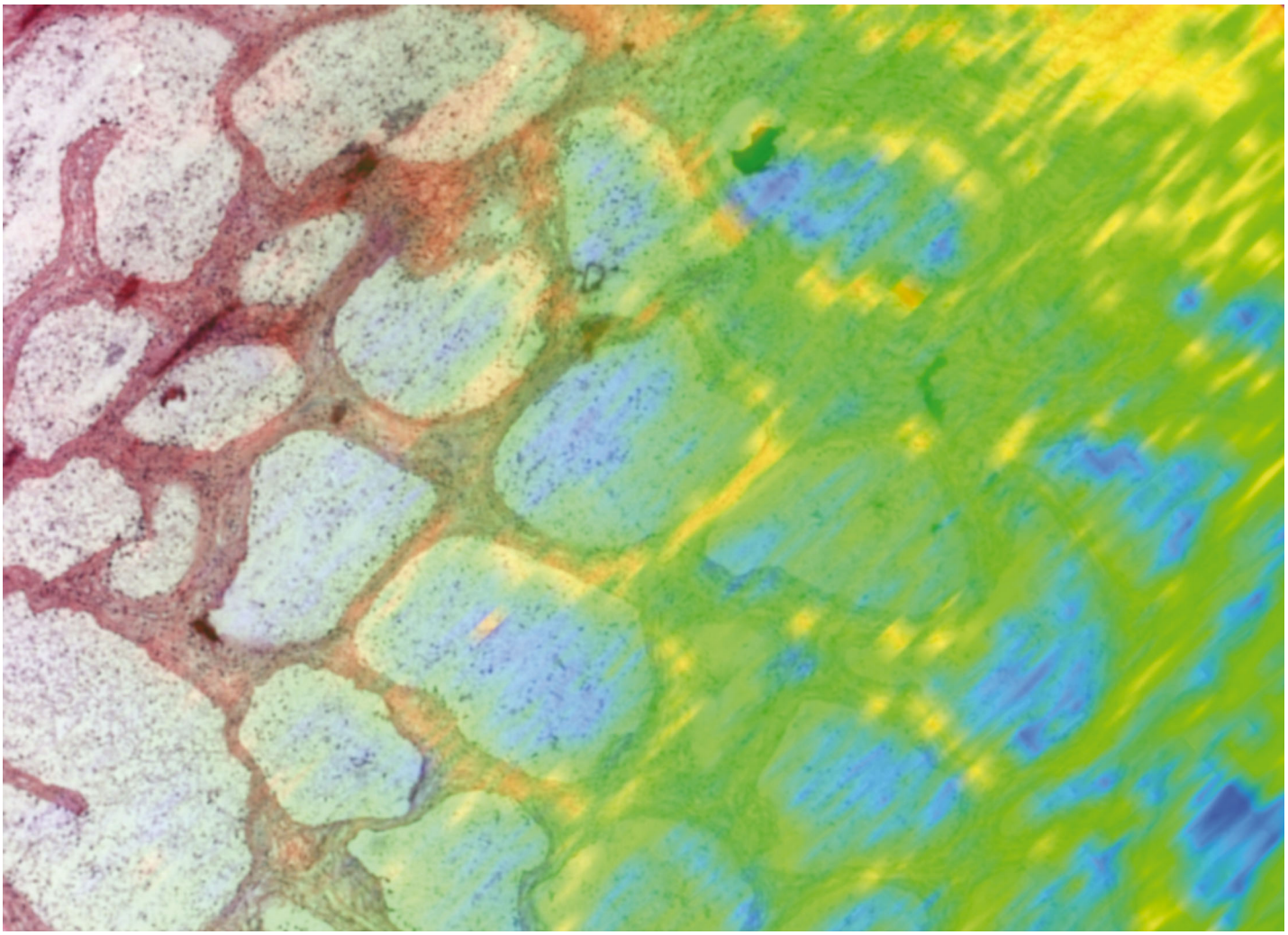

Showcasing research from Professor David Bernhard's laboratory, Division of Pathophysiology, Johannes Kepler University Linz, Upper Austria, Austria.

Chemical imaging and assessment of cadmium distribution in the human body

The image shown is an overlay of light microscopy of haematoxylin–eosin stained sections of human testis (left) and cadmium bioimaging of the same tissue (right). The low concentrations of Cd (blue) within the seminiferous tubules (white-grey zones) and the higher concentrations of cadmium (green and yellow) in the Leydig and Sertoli cells (purple tissue surrounding the seminiferous tubules) indicates the function of the blood-testis barrier *i.e.* to protect sperm from hazardous agents.

As featured in:

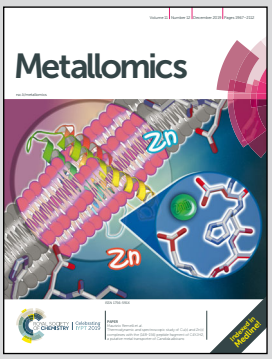

See David Bernhard *et al.*, *Metallomics*, 2019, **11**, 2010.

ROYAL SOCIETY OF CHEMISTRY | Celebrating IYPT 2019

rsc.li/metallomics

Registered charity number: 207890

Metallomics

PAPER

View Article Online
View Journal | View Issue

Cite this: *Metallomics*, 2019, **11**, 2010

Chemical imaging and assessment of cadmium distribution in the human body†

Alexander E. Egger, ‡[ab] Gerlinde Grabmann, ‡[a] Can Gollmann-Tepeköylü,[cd] Elisabeth J. Pechriggl,[d] Christian Artner,[a] Adrian Türkcan,[e] Christian G. Hartinger,[af] Helga Fritsch,[d] Bernhard K. Keppler,[a] Erich Brenner,[d] Michael Grimm,[c] Barbara Messner[e] and David Bernhard*[cgh]

Received 10th July 2019,
Accepted 6th September 2019

DOI: 10.1039/c9mt00178f

rsc.li/metallomics

The scientific interest in cadmium (Cd) as a human health damaging agent has significantly increased over the past decades. However, particularly the histological distribution of Cd in human tissues is still scarcely defined. Using inductively coupled plasma-mass spectrometry (ICP-MS), we determined the concentration of Cd in 40 different human tissues of four body donors and provided spatial information by elemental imaging on the microscopic distribution of Cd in 8 selected tissues by laser ablation (LA)-ICP-MS. ICP-MS results show that Cd concentrations differ by a factor of 20 000 between different tissues. Apart from the well know deposits in kidney, bone, and liver, our study provides evidence that muscle and adipose tissue are underestimated Cd pools. For the first time, we present spatially resolved Cd distributions in a broad panel of human soft tissues. The defined histological structures are mirrored by sharp cut differences in Cd concentrations between neighboring tissue types, particularly in the rectum, testis, and kidneys. The spatial resolution of the Cd distribution at microscopic level visualized intratissue hot spots of Cd accumulation and is suggested as a powerful tool to elucidate metal based toxicity at histological level.

Significance to metallomics

New deposits of Cd in human bodies were discovered by analyzing 40 tissue types per body donor. Cd bioimaging of tissues being involved in the pharmacokinetics and pharmacodynamics (rectum, aorta, liver, and kidney) as well as in the formation of protective barriers (testis) identified the histological structures which are suited best for further studies on the toxicity of Cd at the cellular level.

Introduction

Due to the detrimental effects of cadmium on health, it is of growing scientific and medical interest. The distribution of Cd in human tissues and organs – being the basis for relevant *in vitro* and *in vivo* animal studies – is still not sufficiently characterized. Particularly, the Cd concentrations in different cell types and layers of tissues are insufficiently analyzed.

A limited number of studies have assessed the total human body burden of Cd. Pioneering work in this field stems from studies published from the late 1950ies,[1–4] and an excellent overview was given by Kjellström in 1979.[5] Total body burden and Cd turnover was previously estimated in subjects being chronically exposed to Cd for a long term or experienced acute intoxication. Thus, the concentration of Cd was determined in air, tobacco, nutrition, faeces, *etc.*, and tissues, like kidney, liver, muscle, blood, and pancreas. The total non-occupationally exposed body burden of Cd was estimated to be 30 mg in the "standard American man", 10–18 mg in the European man, and 40–48 mg in Japanese men in "non-polluted areas".[6] Relevant studies were performed on bodies of persons who died from sudden or accidental deaths.[3–5] An important summary on Cd

[a] *Institute of Inorganic Chemistry, University of Vienna, Vienna, Austria*
[b] *ADSI – Austrian Drug Screening Institute GmbH, Innsbruck, Austria*
[c] *Cardiac Surgery Research Laboratory, University Clinic for Cardiac Surgery, Medical University of Innsbruck, Innsbruck, Austria*
[d] *Division of Clinical and Functional Anatomy, Department of Anatomy, Histology and Embryology, Medical University of Innsbruck, Innsbruck, Austria*
[e] *Cardiac Surgery Research Laboratory, Vienna Medical University, Vienna, Austria*
[f] *University of Auckland, School of Chemical Sciences, Auckland, New Zealand*
[g] *Center for Medical Research, Johannes-Kepler-University Linz, Krankenhausstrasse 7a, A-4020 Linz, Austria. E-mail: david.bernhard@jku.at; Tel: +43 73224683080*
[h] *Division of Pathophysiology, Institute of Physiology and Pathophysiology, Medical Faculty, Johannes-Kepler-University Linz, Linz, Austria*

† Electronic supplementary information (ESI) available. See DOI: 10.1039/c9mt00178f

‡ These authors contributed equally to this work.

concentrations in organs and tissues by country was provided by Elinder in 1985.[7] Saltzman *et al.* investigated Cd (as well as Cu, Zn, and Pb) in 26 human cadavers and significantly extended the number of tissues studied to 29.[8] Highest concentrations of Cd were found in the kidney, followed by liver, thyroid, and adrenals as has been shown in previous studies. An interesting outcome of this study was that blood Cd determination must not be performed after death, as blood Cd increases dramatically due to cell lysis or release phenomena.

In addition to the above-mentioned examples of more generalized studies, there exist a number of reports where Cd concentrations were determined in more specific and disease-oriented settings. Mortada *et al.* investigated the role of Cd (as well as Pb and Hg) in cigarette smoke on markers of nephrotoxicity in a relatively young study group (mean age 30 years). They concluded that metal concentrations in cigarette smoke are too low to induce toxicity. However, it was suggested that smoking may be a problem in the presence of other risk factors or pre-damaged kidneys.[9] Cd is well known to damage kidney proximal tubule cells and to be a significant risk factor for kidney failure, given a high level of exposure.[10,11] Cd is also known to be a carcinogen[12] and to reduce bone mineral density. While high levels of Cd exposure cause itai–itai disease,[13] slight increases in environmental exposure to Cd are not thought to reduce bone mineral density.[14] Interestingly, Cd deposition in kidneys of Japanese people who died of itai–itai disease (95 individuals) was significantly lower than in Japanese people who died of other reasons (cortex: 31.5 *vs.* 82.7 $\mu g\ g^{-1}$, respectively) while the concentration in the liver was higher in the exposed group (60.2 *vs.* 8.1 $\mu g\ g^{-1}$).[15] Abu-Hayyeh *et al.* reported on the concentration of Cd in the aorta of smokers, and found the Cd levels to correlate with pack-years smoked.[16,17] The Cd concentrations were found to induce morphological changes and cell death in primary endothelial cells.[18] In the same study, a slight increase in *per se* low levels of serum Cd in young study subjects increased the odds ratio for early atherosclerotic changes in the carotid artery.[18,19]

In order to better understand the underlying mechanisms causing this multitude of adverse effects of Cd on human health, detailed knowledge on the distribution of Cd in tissue is important. So far, the total Cd body burden and the concentration of Cd in organs and tissues have been studied. However, the cell and tissue type specificity of Cd accumulation remains essentially unknown. Only few organs have been analyzed with respect to cell layer specific Cd accumulation, for instance, the well know difference in the concentration of Cd between kidney medulla and cortex (*e.g.* ref. 8), or the differences between the layers of the aortic vessel wall.[16]

Modern techniques have become available to obtain spatially resolved elemental distributions without the need to mechanically separating cell layers. Instead, tissue sections can be analyzed by synchrotron X-ray fluorescence (SXRF) imaging or laser ablation inductively coupled plasma mass spectrometry (LA-ICP-MS) imaging to record elemental distributions in the μm scale.[20,21] Up to now, there are only few examples for mass spectrometric Cd imaging: studies on Cd deposition in human teeth[22] and in human fibrotic and cirrhotic liver tissue,[23] and an investigation of rat placenta to track Cd uptake of the fetus.[24]

With this study we seek to define relevant and potentially new Cd pools in the human body by extending the number and selection of tissues analyzed for their Cd content and to resolve the spatial distribution of Cd at microscopic levels in testis, liver, kidney, rectum, ovary, aorta, and pancreas.

Methods

Study design

The present study is a cadaveric study on four human bodies (2 males/2 females) by people who had given their informed consent prior to death for the use of their bodies for scientific and educational purposes by the Division of Clinical and Functional Anatomy, Department for Anatomy, Histology, and Embryology of the Medical University of Innsbruck, Austria.[25,26] The signed informed consent forms are on hand at the above institution, and this study is in line with the Helsinki-declaration.

This study used non-embalmed fresh bodies with a maximum post mortem time of 48 hours. Body donor characteristics are given in Table 1. Extracted tissue pieces had an approximate size of 5 × 5 × 5 mm. After extraction of tissues, the samples were snap frozen in liquid nitrogen and stored at −80 °C. Tissue samples were further subjected to ICP-MS, LA-ICP-MS, and histological analyses.

Extraction of tissue pieces

Organs were removed and weighed prior to sample excision using a commercially available floor scale (Uwe, Bullseye Scale Company, Sylmar, CA).

Nervous system. After skull trepanation, grey matter from the anterior area of the frontoparietal lobe was obtained. Spinal cord tissue was extracted after diversion of cervical vertebrae. Femoral triangle was dissected for obtaining the femoral nerve distally from its passage through the muscular lacuna.

Skin. Skin tissue was sampled from the ventral side of the forearm. For obtaining mucosa, samples from the respiratory nasal part as well as oral cavity proper were obtained.

Cardiovascular system. Tissue from the anterior wall of the left ventricle was extracted. Arterial samples were obtained from the aortic root, abdominal aorta (next to renal arteries), and femoral artery in the femoral triangle. In addition, tissue from the inferior vena cava in proximity to the right atrium and femoral vein in the femoral triangle was sampled.

Respiratory system. Regarding the trachea, cartilage as well as mucosa proximal of its bifurcation was obtained. In addition, samples from the right upper pulmonary lobe were taken.

Genitourinary system. Kidneys were sampled for cortex as well as medulla. Urinary bladder tissue was obtained from its apex. Testicular tissue was extracted after the dissection of its layers and the scrotum. Ovarian tissue was obtained from the medulla and cortex. Anterior wall of the uterine corpus was sampled.

Gastrointestinal system. Stomach tissue from its corpus was extracted along the greater curvature. Jejunal tissue was obtained distal of the duodenal-jejunal junction. Colon samples were

Table 1 Biomedical characteristics of body donors

	Donor 1	Donor 2	Donor 3	Donor 4
Sex	Male	Male	Female	Female
Race	Caucasian	Caucasian	Caucasian	Caucasian
Age at death [years]	66	64	93	74
Constitution	Obese	Cachectic	Obese	Athletic
Body height [cm]	175	195	160	171
Body weight [kg]	120	85	80	85
Total cholesterol [mg dl^{-1}]	Unknown	167	223	257
HDL cholesterol [mg dl^{-1}]	Unknown	39	51	Unknown
LDL cholesterol [mg dl^{-1}]	Unknown	112	143	Unknown
Smoking status	Unknown	Unknown	Non-smoker	Non-smoker
Profession	Unknown	Unknown	Ward nurse	Housewife
Cause of death	Multi organ failure in hepatic-renal syndrome	Myocardial infarction	Myocardial infarction	Bladder carcinoma
Other characteristics/ indications	History of tuberculosis; hepatocellular carcinoma; liver failure; hepatorenal syndrome.	History of tuberculosis; liver cirrhosis; history of subarachnoidal bleeding; chronic obstructive pulmonary disease; history of gastric surgery.	Peripheral artery disease; clostridial infection; lower leg amputation.	Metastatic bladder carcinoma.

taken from the transverse colon oral to the splenic flexure. Rectum samples were extracted aboral to the sigmoidrectal junction. Tissue from the right hepatic lobe was sampled next to the inferior margo. Gall bladder tissue was obtained from its body. Tissue from the head of pancreas was extracted.

Skeletomuscular system. Bone samples were taken from the ribs, whereas cartilage was obtained from costal cartilage. Muscular tissue was taken from the vastus medialis.

Further tissue. The lens was extracted for further analysis. Finger nail samples were obtained sampling index finger nail. Lymph node samples were taken from the femoral triangle area. In addition, spleen tissue was obtained laterally of the splenic hilum. Thoracic fat samples were taken laterally of the mammary glands. Abdominal fat was obtained from the para-umbilical area. Bone marrow was sampled from ribs.

Quantification of tissue Cd concentrations by ICP-MS

After sample extraction, samples were stored at −20 °C and quantification of Cd was conducted as follows: the wet sample tissue (approx. 30 mg) was digested in quartz vessels with 2 ml of 32.5% HNO_3 (Sigma Aldrich, analytical grade further purified with subPUR/duoPUR, MLS GmbH, Leutkirch, Germany) using a microwave irradiation unit (Discover SP-D, CEM Microwave Technology, Germany). The microwave parameters were as follows: temperature and maximal power were set to 200 °C and 300 W, respectively, with a ramp time of 4 min, a hold time of 6 min and 3.5 min cooling time until the temperature reached 80 °C. Only a single digestion was feasible for fingernail and eye lens due to very low sample amounts. All other samples were prepared in duplicates or triplicates (see below). The digested samples and the microwave blanks were diluted with high-purity water (Milli-Q Advantage A10, Merck Millipore, Darmstadt, Germany) to a total weight of approx. 10 g. The quantification of cadmium was performed on an ICP-MS instrument (QQQ 8800, Agilent Technologies, Tokyo, Japan) registering the isotopes ^{111}Cd (analyte) and ^{115}In (internal standard). A detailed list of instrumental setup and parameters is given in Table S1 (ESI†). Standard stock solutions were purchased from CPI International (Santa Rosa, USA) and diluted with 3.2% HNO_3 yielding final concentrations in the range of 0.01–25 ng g^{-1} Cd for the calibration curve. If the two determinations deviated by more than 25% from each other the samples were considered inhomogeneous and a third digestion was conducted. In that case, all three values were used to calculate the Cd concentration (arithmetic mean) of each sample.

The limit of detection was determined by measurement of $n = 10$ digestion blanks, resulting in a procedural limit of detection (3s-criterion) and quantification (10s-criterion) of 9 pg g^{-1} and 13 pg g^{-1} in solution. After 12 samples a solution blank and a standard were measured to monitor the stability of the instrument which showed reproducible results (2% RSD) throughout all measurements. Additionally, a Clincheck® Controls serum for trace elements (Recipe, Munich, Germany) was prepared according to the instructions and treated as the samples. The concentration found was within the control range.

In order to check the accuracy of the entire method, a certified reference material (human hair, NIES, CRM No. 13, Environmental Agency, Japan) underwent the same procedure as the samples ($n = 3$). The Cd concentration determined in the CRM was 220 ± 8 μg kg^{-1} ($n = 3$) which equals a recovery of 96% (certified value: 230 ± 30 μg kg^{-1}).

Assessment of the relative distribution of Cd in four human cadavers

To assess the relative distribution of Cd in the cadavers, results from ICP-MS analysis were combined with corresponding organ weights as follows: organs, with a defined weight (not for all cadavers – see below), included heart, kidneys, liver, lung, and spleen. Organ/tissue weight calculations were performed according to the algorithms developed by Young *et al.* and Luecke *et al.*[27,28] and covered the following organs and tissues: adipose, bone marrow, brain, breast, heart, intestines, kidneys, liver, lung, mammary, muscles, pancreas, skin, spleen, stomach, and testis. For donor 4, all organ weights were calculated, as was the weight of the spleen of donor 2. To obtain the total amount of Cd in an organ/tissue (calculated or

weighed), the individual organ/tissue mass (in kg) was multiplied by the Cd concentration of the organ/tissue (μg kg^{-1} – data from Table 2). Further, the sum of weights of all the organs/tissues mentioned above was set relative to the body weight of the donor and is expressed as percent of the body weight.

Spatially-resolved Cd distribution by LA-ICP-MS

Sample preparation. LA-ICP-MS was conducted on cryo-sections (20 μm) embedded in Tissue-Tek® (Sakura Finetek, The Netherlands) of representative samples originating from liver, kidney (cortex and cortex-medulla border zone), aorta, ovary, pancreas, rectum, and testis. LA-ICP-MS imaging was conducted on the tissue samples with the highest Cd concentration (as determined by acid digestion). In order to correlate the Cd distribution with histologic features, a consecutive section (5 μm) was stained with haematoxylin and eosin and mounted in Eukitt quick hardening mounting medium. Images were produced using a Zeiss microscope equipped with the Axio-Software to produce MosaiX images of the organs.

Table 2 Cd concentrations in tissue samples. All concentrations are given in [μg kg^{-1}]. Cd concentrations of the four donors (#1–#4) are average values of at least two independent measurements (except finger nail and lens). Kidney medulla and cortex of donor 4 were not separated. See material and methods for details of the sample preparation

	Tissue concentration, μg kg^{-1}				
Tissue type	Median	#1, m	#2, m	#3, f	#4, f
Lens	6.5	1.35[a]	18.4	n.a.	6.48
Fingernail	20	16.6	45	24.3	12.3
Bone (rib)	24	22.9	92.0	25.4	10.2
Spinal marrow	25	22.3	n.a.	n.a.	26.7
Cerebral cortex	25	38.9	43.2	65.6	13.2
Skin	26	17.9	95.1	22.6	28.7
Nerve (ischiadicus)	31	31.6	167	n.a.	22.5
Adipose tissue (breast)	32	47.2	45.4	18.7	7.29
Heart muscle	35	22.7	72.6	21.8	46.4
Nasal mucosa	36	30.8	142	27.9	41.4
Cartilage (rib)	36	7.32	38.2	34.5	41.2
Oral mucosa	40	36.2	141	44.0	26.0
Bladder	41	n.a.	n.a.	59.0	23.0
Adipose tissue (waist)	42	9.60	74.5	78.5	9.71
Cartilage (trachea)	46	n.a.	n.a.	n.a.	46.4
Spleen	48	22.3	n.a.	n.a.	73.7
Prostate	55	54.6	n.a.	—	—
Bone marrow	55	20.5	86.2	199	24.1
Lymph node	56	31.4	160	80.6	24.5
Vein (radial)	62	16.0	130	62.7	n.a.
Artery (radial)	63	24.6	222	90.2	35.7
Trachea	64	68.3	254	60.3	51.4
Retina	73	n.a.	n.a.	73.0	n.a.
Vein (cava)	76	75.8	n.a.	52.3	91.5
Diaphragm	88	95.9	296	81.4	49.9
Aorta (ascendens)	94	n.a.	160	52.3	94.7
Small intestine	100	63.1	566	145	52.9
Rectum	106	106	369	35.3	n.a.
Large intestine	110	106	301	55.8	108
Uterus	120	—	—	118	n.a.
Stomach	120	52.1	255	82.8	153
Lung	130	53.5	377	51.4	208
Skeletal muscle	170	n.a.	242	n.a.	107
Aorta (abdominal)	200	237	52.3	562	165
Pancreas	240	7.54	n.a.	n.a.	466
Ovary	270	—	—	267	n.a.
Testis	340	110	565	—	—
Liver	750	106	1030	483	1230
Kidney medulla	5100	3970	28 600	2400	6280[b]
Kidney cortex	6800	6170	28 300	7300	

[a] Indicates a detectable amount of Cd (but below limit of quantification). It is still stated to retrace the calculation of the median. [b] Medulla and cortex were not separated in donor 4. n.a. not available. — sex specific organ.

LA-ICP-MS. Laser ablation was performed with a Nd:YAG solid state laser (NWR213, ESI, Fremont, CA, USA) at a wavelength of 213 nm, equipped with a 2 volume ablation cell to reduce the wash out time. The laser was operated at 10 Hz, with a fluence in the range of 3.0 to 3.2 J cm^{-2}, a square-shaped spot size of 70 μm, a scan speed of 40 μm s^{-1}, a warm up time of 10 s and a wash out delay of 12–15 s. The spacing between the parallel line scans was 10 μm.

Helium (5.0) at a flow rate of 400 mL min^{-1} was used to transfer the ablated material to the ICP-MS. The ICP-MS was operated in Single Quad mode at an RF-power of 1350 W, argon plasma gas of 15 L min^{-1}, and carrier gas of 1.07 L min^{-1} to record ^{111}Cd and ^{114}Cd with dwell times of 0.1 and 0.2 s, respectively. The eight samples were measured within two consecutive days in order to ensure stable LA-ICP-MS conditions.

Data analysis. The software Igor Pro (Wavemetrics, Igor Pro 6.34A) together with the add-on Iolite (Iolite Version 2.5, University of Melbourne) was used for generating ^{114}Cd distribution maps.[29] The data reduction scheme 'Trace_Elements' including blank subtraction was applied. The reliability of the LA-ICP-MS data was verified by calculating the median counts per second (cps) of each tissue section *via* histograms and corresponding box-plots of a greyscale Cd distribution, using ImageJ (Version 1.48v) and Matlab (Version 2014a), respectively (Fig. S1, ESI†). These values were plotted against quantitative data (μg kg^{-1}) of the same sample obtained from microwave-assisted digestion followed by ICP-MS analysis (Fig. 2).

Results and discussion

Cd concentrations in human organs and tissues

The pattern of Cd deposition in the body of non-occupationally exposed humans in central Europe (province of Tyrol, Austria) was studied. Samples of 40 different tissues from 4 bodies (2 males, 2 females) with a median age of 70.5 years (range 64–93) were collected as described above. Microwave-assisted digestions of the tissue samples were followed by ICP-MS analysis to quantify Cd. Some samples were either small in size (*e.g.* retina or lens) and/or possessed only low concentrations of Cd that challenged quantification (Table 2).

The lowest concentration of Cd in all tissues analyzed was found in the lens of donor 1 (approx. 1.35 μg kg^{-1}, <LOQ). Generally, tissues with low blood perfusion, like lens, finger nail, bone, cartilage, nerve, and adipose, showed low concentrations of Cd. Interestingly, tissues like brain, nasal and oral mucosa, heart muscle, and skin were also among the tissues with low Cd concentration (median <50 μg kg^{-1}). An intermediate Cd concentration (median between 50 and 150 μg kg^{-1}) was found, in ascending order, in immune-relevant organs/tissues, blood

vessel, the gastro-intestinal system, and lung. High concentrations of Cd (median >150 μg kg^{-1}) were found in skeletal muscle (170 μg kg^{-1}), abdominal aorta (200 μg kg^{-1}), ovary (270 μg kg^{-1}), and testis (340 μg kg^{-1}). The median concentration of Cd in liver was 750 μg kg^{-1}. By far the highest concentration of Cd was found in kidney tissue (median concentration kidney medulla 5100 μg kg^{-1}, cortex 6800 μg kg^{-1}). The highest Cd concentration of all analyzed tissues was found in the kidney cortex of donor 2 and was 20 000-fold higher (28 300 μg kg^{-1}) than the lowest concentration in the lens of donor 1, showing a wide bandwidth of Cd concentrations in different tissue types. Previous studies of organs indicate that epidemiologically relevant Cd concentrations are defined by gender, age, smoking habit, and disease.[30–32]

The interconnection between high serum cholesterol levels, which multiply Cd deposition in kidney and myocardium observed in mice, may also be of interest.[33] In our study, donors 3 and 4 had high levels of cholesterol (223 and 257 mg dl^{-1}, respectively). However, Cd concentration in heart muscle (21.8 and 46.4 μg kg^{-1}, respectively) and kidney cortex (7300 and 6280 μg kg^{-1}, respectively) as well as total Cd in the respective tissues (see next section, Fig. 1) were lower compared to donor 2 (serum cholesterol 167 mg dl^{-1}, Cd concentration in heart muscle and kidney cortex 72.6 and 28 300 μg kg^{-1}, respectively).

In a next step we calculated individual Cd distribution patterns for each donor aiming to discover new Cd pools. We also determined spatially resolved Cd distribution patterns of selected tissue types by means of LA-ICP-MS.

Relative Cd distribution in the human body

The relevance of a Cd pool is defined by concentration and size. Based on measurements of organ weight and algorithm-based organ weight estimations,[27,28] (see Experimental section for details) major deposits of Cd in the donors could be identified (see Fig. 1). Importantly, the size of Cd pools has a significant variability between the donors, which may in part be caused by organ size estimations. A high degree of variability between individuals can also be caused by their history in terms of smoking habits as this is a known source for Cd exposure, for example.[34] Unfortunately no information on the smoking status was available in the records of donor 1 and 2. We refrained from histological evaluation, *e.g.* of lung tissue, as there are many other environmental impacts such as exhaust fumes causing similar depositions as smoking.[35] Nevertheless, the most important Cd pools in the donors were identified as the kidneys, muscle, adipose tissue, liver, and bone marrow. As no samples were available for muscle in the case of donors 1 and 3, the covered analysed body weight is reduced to approx. 50% in these two cases. The amount of Cd in kidney is high compared to its size. Muscle and adipose tissue are very large in size but hold only a low Cd concentration, underestimating their relevance as a Cd pool. Based on our own and the data reported by Saltzman *et al.*,[8] bone has similar or less Cd concentrations compared to skeletal muscle. Since body muscle mass is almost three times higher compared to body bone mass, it can be estimated that the body bone Cd pool makes up <8% of the total human body Cd.

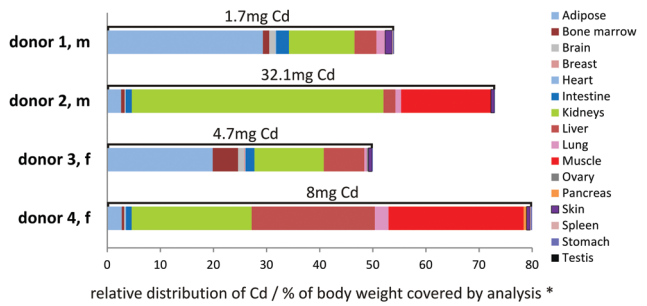

Fig. 1 Relative distribution of Cd in four body donors. Relative distribution of Cd in various organs and tissues of four human bodies based on Cd concentration values (measured by ICP-MS) multiplied by measured or calculated organ weights. The maximum extent of the bars on the *x*-axis gives the sum of the weight of all organs and tissues covered by the analysis as % of the donor's body weight. The sum of Cd amounts of all organs/tissues, which are covered by the analysis, is given on top of each bar.

Depending on the individual donor, relations between organ Cd pools differ significantly. The largest Cd pool in donors 1 and 3 was adipose tissue, followed by kidneys (in the absence of data for Cd in muscle). The central Cd pool was kidney in donor 2, who also possessed by far the highest body burden of Cd (32 mg) in 75% body weight covered by analysis. In the case of the other donors, 50–80% of the total body weight was covered yielding to a total Cd burden of <10 mg within this fraction. In donor 4, approximately equally sized Cd pools were found for kidney, liver, and muscle. Previous studies already suggested that muscle may form an important Cd pool.[3,4] However, the relevance of these pools in the genesis and progression of Cd-dependent diseases and age-related processes is still unclear.

Especially the discovery of adipose tissue as a potentially relevant Cd pool in the human body is an important finding of this study and should be further investigated. This pool may have been underestimated in the past due to its low Cd concentration. However, with an increasing mass of adipose tissue (*e.g.* caused by nutritional behaviours, physical inactivity, or ageing) adipose tissue turns into one of the biggest Cd pools of the entire body as already observed in our study for the obese donors 1 and 3 compared to the non-obese individuals 2 and 4. In addition, humans develop signs of Cd related diseases already at many-fold lower concentrations compared to mice and rats,[33] indicating the importance to focus on tissue with low concentrations of Cd in human studies.

Clearly, the form in which Cd is applied and present *in vivo*, shall be a subject of intensive research of the coming years as intracellular Cd concentrations are dependent on the equilibrium between cellular/tissue uptake, storage, and export.

It is well known that in biological systems Cd is almost completely bound to and transported by proteins, like albumin or metallothioneins.[36] A significant number of studies have been published showing the enormous complexity and cell type specificity of Cd-binding proteins, channels, and transporters.[36–39]

Therefore, we were interested in the spatial distribution of Cd within tissue sections at microscopic level and analysed tissue sections using a bioimaging approach by means of LA-ICP-MS.

Bioimaging of Cd and correlation with histology

Eight tissues were additionally subjected to LA-ICP-MS analysis: abdominal aorta, kidney medulla, kidney cortex (all taken from donor 1), rectum, testis, liver (all taken from donor 2), ovary (donor 3), and pancreas (donor 4). These organs are typically involved in pharmacokinetics and contain a high average concentration of Cd. First, the LA-ICP-MS data (cps) was correlated with the absolute Cd concentration (μg kg^{-1}) obtained by analysis of digested samples (Fig. 2). The resulting "calibration" (R^2 = 0.9924) revealed that averaging over the entire distribution in a tissue section provides comparable data to the average concentration determined by microwave-assisted digestion followed by ICP-MS analysis. We found the following correlation to estimate the spatially resolved Cd concentration (in μg kg^{-1}) in tissue samples:

$$c(\text{Cd, } \mu\text{g kg}^{-1}) = 1.23 \times \text{cps(Cd)} - 9.1 \quad (1)$$

Next, we correlated the Cd distributions with histologic features of the tissue sections: Fig. 3 and 4 depict the Cd distribution (left), the grey scale image of the sample prior to ablation (middle), and a consecutive, HE-stained slice (right). The rectum sample (Fig. 3, top) allows clear distinction between three histological layers in the HE stained section (from left to right): the mucosa, the submucosa, and the tunica muscularis. The corresponding LA image shows that the tunica muscularis contains approximately twice the amount of Cd compared to the other two layers. This finding may be of interest for future examinations of Cd transport and deposition in the rectum. The aortic wall specimens (Fig. 3, 2nd row) did not show clear wall layer-dependent differences in Cd deposition (left to right: adventitia, media, and intima). Even though an increased concentration of Cd in the media of the infra renal aorta was reported in the literature, we could not observe this.[16] The ovary (Fig. 3, 3rd row) which displayed a menopausal state (rich in connective tissue, no clear signs of cyclic activity) was characterized by a relatively even spatial distribution of Cd. Similarly, we could not observe differences in Cd deposition which would reflect the architecture of the pancreas (Fig. 3, bottom row). The lobes of the exocrine pancreas did not differ from connective tissue, interlobular excretion ducts, or Langerhans islets. Only larger blood vessels in the connective tissue outside the pancreas showed increased levels of Cd. The upper row images in Fig. 4 show the analysis of the testis of donor 2. LA-ICP-MS analysis (left side) gave a good impression on the functions of the blood-testis barrier regarding Cd transition and deposition. The convoluted seminiferous tubules displayed relatively low Cd levels (200–250 cps) while the surrounding Sertoli cells (blood-testis barrier) had significantly higher levels of Cd (~750 cps). Intermediate Cd levels were found in connective tissue (surrounding the Sertoli cells) containing blood vessels and Leydig cells (500–600 cps). Cd has been shown to reduce the function of Sertoli cells (Cd reduces the production of inhibinB, AMH, and FSH[40,41]), leading to a gradual loss of Sertoli barrier function and at very high concentration can cause haemorrhage.

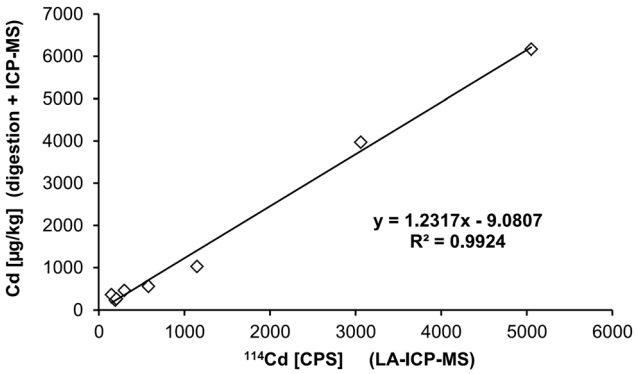

Fig. 2 Correlation of LA-ICP-MS median cps values and microwave-assisted digestion ICP-MS. Identical tissue samples (*i.e.* from the same donor) were analysed by both methods.

Out of the three tissues with the highest Cd concentration, *i.e.*, the liver, kidney medulla, and kidney cortex, the liver showed a relatively homogenous distribution of Cd (Fig. 4, 2nd row). Histological structures were hardly reflected by differences in Cd deposition. The kidney, as the organ comprising by far the highest concentration of Cd, was analysed twice using LA-ICP-MS. Row 3 of Fig. 4 shows the border zone between the kidney medulla and the cortex, where significant differences in Cd concentrations between cell layers were observed. It has to be mentioned here, that we could previously show an influence of tissue type on LA-ICP-MS signals; *i.e.* in a LA-ICP-MS study of platinum deposition it was found that concentrations in adipose tissue are underestimated.[42] Whether or not this finding is also applicable to Cd analyses in adipose tissue remains to be determined. The analysis of kidney cortex (Fig. 4 bottom row) showed that the cortex had by far the highest concentrations of Cd and also that Cd was evenly distributed throughout the sample.

It was previously reported that Cd is enriched in the kidney cortex which can be approximated by multiplying the Cd concentration of the whole kidney by a factor of 1.25.[43] Our study is in accordance with this finding, as the average concentration in the cortex is approx. 1.32 higher than in the medulla. Generally, the Cd concentration in the kidney cortex was higher than in the medulla or other kidney compartments because Cd which is protein bound in the circulation like other metals, can freely pass into the glomerular filtrate. Protein–Cd complexes are then absorbed into the cells of the proximal convoluted tubules where Cd is released and consequently binds to *e.g.* metallothioneins, which leads to an accumulation of Cd in the kidney cortex.[44]

Our study covered the largest number of tissue samples per body donor so far, *i.e.* 38 to 40 tissues per donor. Quantification of Cd with ICP-MS and additional imaging of organs involved in uptake (intestine), transport (aorta), metabolism (liver),

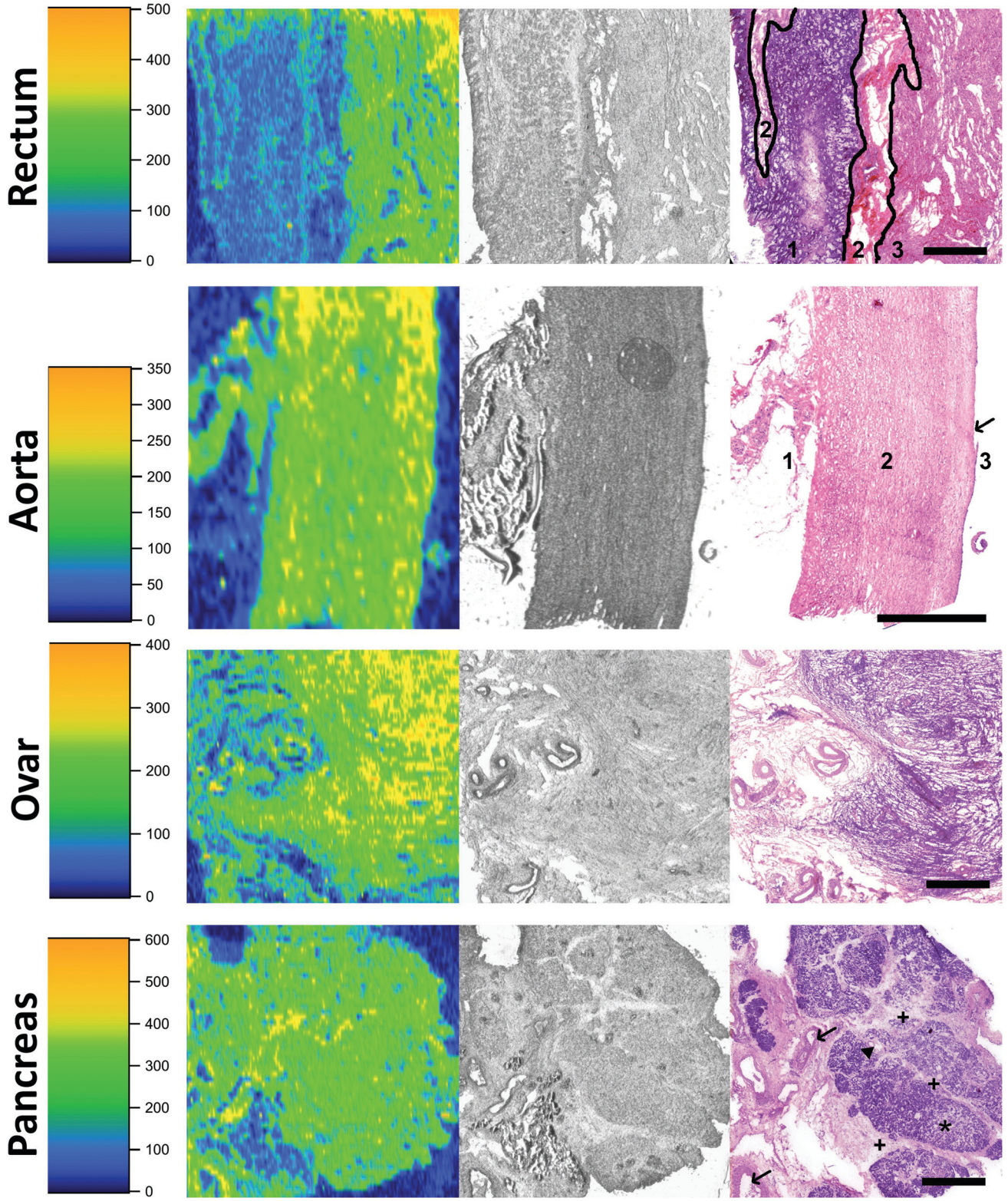

Fig. 3 Cadmium bioimaging in tissue sections of rectum (donor 2), aorta (donor 1), ovary (donor 3) and pancreas (donor 4). Left column: LA-ICP-MS for cadmium, middle row: unstained sections prior to ablation, right column: HE-stained consecutive sections. Scale bars indicate 1 mm. Top row (rectum), right image: mucosa (1), submucosa (2), tunica muscularis (3). The boarders between these layers are indicated by drawn lines. Second row (aorta), right image: adventia (1), media (2), vessel lumen (3), vascular endothelium (intima, →). Third row (ovary), right image: menopausal state, mostly characterized by connective tissue. Bottom row (pancreas), right image: connective tissue (+), glandular lobes of the exocrine pancreas (*), interlobular excretion duct (▲), blood vessels in connective tissue (→).

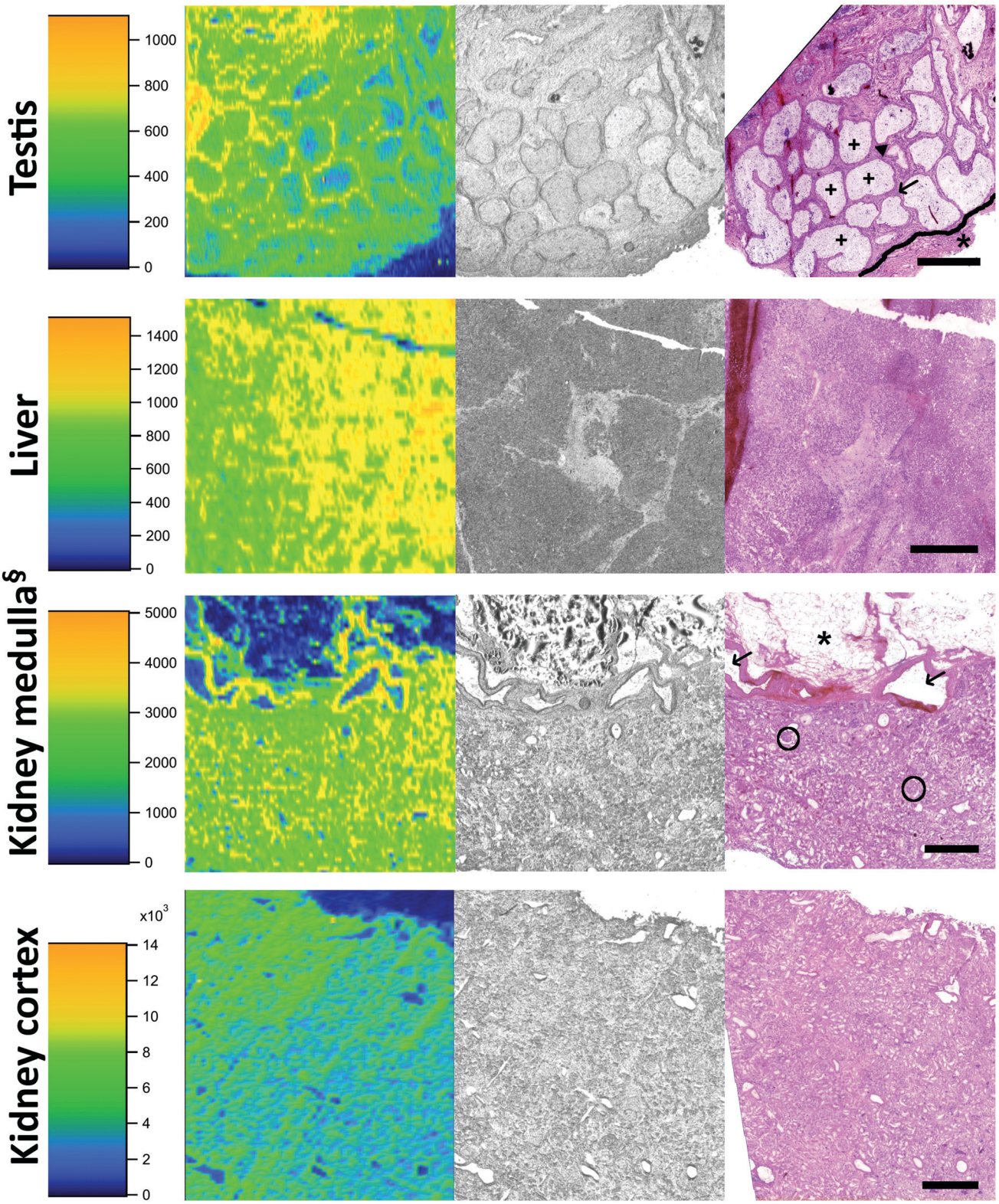

Fig. 4 Cadmium bioimaging in tissue sections of testis (donor 2), liver (donor 2), kidney medulla-cortex boarder (donor 1), and the kidney cortex (donor 1). Left column: LA-ICP-MS of cadmium, middle row: unstained sections prior to ablation, right column: HE-stained consecutive sections. Scale bars indicate 1 mm. Top row (testis): convoluted seminiferous tubules (+), tunica albuginea (*), Leydig cells (▲), Sertoli cells (→). Third row (medulla): § – this section shows the medulla/cortex boarder zone; bowman capsule with glomeruli (O), blood vessels (→), adipose and connective tissue (*).

excretion (kidney), reproduction (testis, ovary) provide a first impression on the intratissue distribution of Cd within one body.

Conclusions

Quantitative determination of the average Cd concentration in human body tissue combined with spatially resolved visualization of the Cd distribution in tissue sections gave a comprehensive picture on the location of Cd in four human body donors. We ranked the identified Cd pools by the concentration in the respective tissue and by their mass. We concluded that adipose tissue or muscle tissue – despite bearing low concentrations of Cd – represent an important pool for the total Cd burden due to their large fraction on the total body weight.

Laser ablation ICP-MS bioimaging experiments were undertaken for the first time on a broader panel of human tissues and we obtained new insights into the intra-tissue distribution of Cd. Unevenly distributed patterns in rectum, kidney, and testis were discovered. These tissues are responsible for uptake, excretion, and formation of barriers (*e.g.* blood-testes barrier). The discovered areas of Cd accumulation are the corner stone for subsequent (sub)cellular imaging of Cd (*e.g.* glomerula of kidneys) to further extend the knowledge on processes involved in Cd metabolism and toxicity.

Conflicts of interest

There are no conflicts to declare.

Acknowledgements

The authors wish to thank the individuals who donated their bodies and tissues for the advancement of education and research.[25,26] This study was supported by the Austrian National Bank (OeNB grant 14745 to D. B., and 14590 to B. M.), the University of Auckland, and the Royal Society of New Zealand to C. G. H., the University of Vienna (PhD scholarship within the doctoral program BioProMoTION (Bioactivity Profiling and Metabolism)) to G. G., and the Tiroler Wissenschaftsfonds (TWF-2016-1-9).

References

1 L. Friberg, Chronic cadmium poisoning, *AMA Arch. Ind. Health*, 1959, **20**, 401–407.
2 G. F. Nordberg and T. Kjellstrom, Metabolic model for cadmium in man, *Environ. Health Perspect.*, 1979, **28**, 211–217.
3 S. S. Salmela, E. Vuori, A. Huunan-Seppala, J. O. Kilpio and H. Sumuvuori, Body burden of cadmium in man at low level of exposure, *Sci. Total Environ.*, 1983, **27**, 89–95.
4 E. Vuori, A. Huunan-Seppala, J. O. Kilpio and S. S. Salmela, Biologically active metals in human tissues. II. The effect of age on the concentration of cadmium in aorta, heart, kidney, liver, lung, pancreas and skeletal muscle, *Scand. J. Work, Environ. Health*, 1979, **5**, 16–22.
5 T. Kjellstrom, Exposure and accumulation of cadmium in populations from Japan, the United States, and Sweden, *Environ. Health Perspect.*, 1979, **28**, 169–197.
6 H. A. Schroeder, A. P. Nason, I. H. Tipton and J. J. Balassa, Essential trace metals in man: zinc. Relation to environmental cadmium, *J. Chronic Dis.*, 1967, **20**, 179–210.
7 C. G. Elinder, in *Cadmium and Health: A Toxicological and Epidemiological Appraisal*, ed. L. E. Fridberg, T. Kjellström and G. F. Nordberg, CRC Press, 1985, vol. 1, pp. 81–102.
8 B. E. Saltzman, S. B. Gross, D. W. Yeager, B. G. Meiners and P. S. Gartside, Total body burdens and tissue concentrations of lead, cadmium, copper, zinc, and ash in 55 human cadavers, *Environ. Res.*, 1990, **52**, 126–145.
9 W. I. Mortada, M. A. Sobh and M. M. El-Defrawy, The exposure to cadmium, lead and mercury from smoking and its impact on renal integrity, *Med. Sci. Monit.*, 2004, **10**, CR112–CR116.
10 N. Johri, G. Jacquillet and R. Unwin, Heavy metal poisoning: the effects of cadmium on the kidney, *Biometals*, 2010, **23**, 783–792.
11 W. C. Prozialeck and J. R. Edwards, Mechanisms of cadmium-induced proximal tubule injury: new insights with implications for biomonitoring and therapeutic interventions, *J. Pharmacol. Exp. Ther.*, 2012, **343**, 2–12.
12 A. Hartwig, Cadmium and cancer, *Met. Ions Life Sci.*, 2013, **11**, 491–507.
13 M. Uetani, E. Kobayashi, Y. Suwazono, R. Honda, M. Nishijo, H. Nakagawa, T. Kido and K. Nogawa, Tissue cadmium (Cd) concentrations of people living in a Cd polluted area, Japan, *Biometals*, 2006, **19**, 521–525.
14 X. Chen, G. Zhu, T. Jin, A. Akesson, I. A. Bergdahl, L. Lei, S. Weng and Y. Liang, Changes in bone mineral density 10 years after marked reduction of cadmium exposure in a Chinese population, *Environ. Res.*, 2009, **109**, 874–879.
15 C. Hayashi, N. Koizumi, H. Nishio, N. Koizumi and M. Ikeda, Cadmium and other metal levels in autopsy samples from a cadmium-polluted area and non-polluted control areas in Japan, *Biol. Trace Elem. Res.*, 2012, **145**, 10–22.
16 S. Abu-Hayyeh, M. Sian, K. G. Jones, A. Manuel and J. T. Powell, Cadmium accumulation in aortas of smokers, *Arterioscler., Thromb., Vasc. Biol.*, 2001, **21**, 863–867.
17 https://www.cancer.gov/publications/dictionaries/cancer-terms/def/pack-year, (accessed 2019-08-26).
18 B. Messner and D. Bernhard, Cadmium and cardiovascular diseases: cell biology, pathophysiology, and epidemiological relevance, *Biometals*, 2010, **23**, 811–822.
19 B. Messner, M. Knoflach, A. Seubert, A. Ritsch, K. Pfaller, B. Henderson, Y. H. Shen, I. Zeller, J. Willeit, G. Laufer, G. Wick, S. Kiechl and D. Bernhard, Cadmium is a novel and independent risk factor for early atherosclerosis mechanisms and in vivo relevance, *Arterioscler., Thromb., Vasc. Biol.*, 2009, **29**, 1392–1398.
20 D. J. Hare, E. J. New, M. D. de Jonge and G. McColl, Imaging metals in biology: balancing sensitivity, selectivity and spatial resolution, *Chem. Soc. Rev.*, 2015, **44**, 5941–5958.
21 A. Sussulini, J. S. Becker and J. S. Becker, Laser ablation ICP-MS: Application in biomedical research, *Mass Spectrom. Rev.*, 2017, **36**, 47–57.

22 D. Hare, C. Austin, P. Doble and M. Arora, Elemental bioimaging of trace elements in teeth using laser ablation-inductively coupled plasma-mass spectrometry, *J. Dent.*, 2011, **39**, 397–403.
23 P. M-M, R. Weiskirchen, N. Gassler, A. K. Bosserhoff and J. S. Becker, Novel bioimaging techniques of metals by laser ablation inductively coupled plasma mass spectrometry for diagnosis of fibrotic and cirrhotic liver disorders, *PLoS One*, 2013, **8**, e58702.
24 Y. Yamagishi, S. Furukawa, A. Tanaka, Y. Kobayashi and A. Sugiyama, Histopathological localization of cadmium in rat placenta by LA-ICP-MS analysis, *J. Toxicol. Pathol.*, 2016, **29**, 279–283.
25 S. McHanwell, E. Brenner, A. R. M. Chirculescu, J. Drukker, H. van Mameren, G. Mazzotti, D. Pais, F. Paulsen, O. Plaisant, M. Caillaud, E. Laforêt, B. M. Riederer, J. R. Sanudo, J. L. Bueno-Lopez, F. Donate, P. Sprumont, G. Teofilovski-Parapid and B. J. Moxham, The legal and ethical framework governing Body Donation in Europe - A review of current practice and recommendations for good practice, *Eur. J. Anat.*, 2008, **12**, 1–24.
26 B. M. Riederer, S. Bolt, E. Brenner, J. L. Bueno-Lopez, A. R. M. Cirulescu, D. C. Davies, R. De Caro, P. O. Gerrits, S. McHanwell, D. Pais, F. Paulsen, O. Plaisant and E. Sendemir, I. Stabile and B. J. Moxham, The legal and ethical framework governing Body Donation in Europe – 1st update on current practice, *Eur. J. Anat.*, 2012, **16**, 1–21.
27 R. H. Luecke, B. A. Pearce, W. D. Wosilait, W. Slikker Jr. and J. F. Young, Postnatal growth considerations for PBPK modeling, *J. Toxicol. Environ. Health, Part A*, 2007, **70**, 1027–1037.
28 J. F. Young, R. H. Luecke, B. A. Pearce, T. Lee, H. Ahn, S. Baek, H. Moon, D. W. Dye, T. M. Davis and S. J. Taylor, Human organ/tissue growth algorithms that include obese individuals and black/white population organ weight similarities from autopsy data, *J. Toxicol. Environ. Health, Part A*, 2009, **72**, 527–540.
29 C. Paton, J. Hellstrom, B. Paul, J. Woodhead and J. Hergt, Iolite: Freeware for the visualisation and processing of mass spectrometric data, *J. Anal. At. Spectrom.*, 2011, **26**, 2508–2518.
30 E. M. Andersson, B. Fagerberg, G. Sallsten, Y. Borné, B. Hedblad, G. Engström and L. Barregard, The association between tobacco smoking and atherosclerotic plaques in the carotid artery is partly mediated by cadmium exposure, *Am. J. Epidemiol.*, 2017, **187**, 806–816.
31 T. G. Kazi, S. K. Wadhwa, H. I. Afridi, N. Kazi, G. A. Kandhro, J. A. Baig, A. Q. Shah, N. F. Kolachi and M. B. Arain, Interaction of cadmium and zinc in biological samples of smokers and chewing tobacco female mouth cancer patients, *J. Hazard. Mater.*, 2010, **176**, 985–991.
32 T. Wei, J. Jia, Y. Wada, C. M. Kapron and J. Liu, Dose dependent effects of cadmium on tumor angiogenesis, *Oncotarget*, 2017, **8**, 44944–44959.
33 A. Turkcan, B. Scharinger, G. Grabmann, B. K. Keppler, G. Laufer, D. Bernhard and B. Messner, Combination of cadmium and high cholesterol levels as a risk factor for heart fibrosis, *Toxicol. Sci.*, 2015, **145**, 360–371.
34 G. Scherer and H. Barkemeyer, Cadmium concentrations in tobacco and tobacco smoke, *Ecotoxicol. Environ. Saf.*, 1983, **7**, 71–78.
35 M. G. Padovan, A. Whitehouse, N. Gouveia, M. Habermann and J. Grigg, Carbonaceous particulate matter on the lung surface from adults living in São Paulo, Brazil, *PLoS One*, 2017, **12**, e0188237.
36 F. Thevenod, Catch me if you can! Novel aspects of cadmium transport in mammalian cells, *Biometals*, 2010, **23**, 857–875.
37 C. D. Klaassen, J. Liu and S. Choudhuri, Metallothionein: an intracellular protein to protect against cadmium toxicity, *Annu. Rev. Pharmacol. Toxicol.*, 1999, **39**, 267–294.
38 L. He, B. Wang, E. B. Hay and D. W. Nebert, Discovery of ZIP transporters that participate in cadmium damage to testis and kidney, *Toxicol. Appl. Pharmacol.*, 2009, **238**, 250–257.
39 S. Segawa, M. Shibamoto, M. Ogawa, S. Miyake, K. Mizumoto, A. Ohishi, K. Nishida and K. Nagasawa, The effect of divalent metal cations on zinc uptake by mouse Zrt/Irt-like protein 1 (ZIP1), *Life Sci.*, 2014, **113**, 40–44.
40 A. Janecki, A. Jakubowiak and A. Steinberger, Effect of cadmium chloride on transepithelial electrical resistance of Sertoli cell monolayers in two-compartment cultures--a new model for toxicological investigations of the ''blood-testis'' barrier in vitro, *Toxicol. Appl. Pharmacol.*, 1992, **112**, 51–57.
41 G. Luca, C. Lilli, C. Bellucci, F. Mancuso, M. Calvitti, I. Arato, G. Falabella, S. Giovagnoli, M. C. Aglietti, A. Lumare, G. Muzi, R. Calafiore and M. Bodo, Toxicity of cadmium on Sertoli cell functional competence: an *in vitro* study, *J. Biol. Regul. Homeost. Agents*, 2013, **27**, 805–816.
42 A. E. Egger, C. Kornauth, W. Haslik, S. Hann, S. Theiner, G. Bayer, C. G. Hartinger, B. K. Keppler, U. Pluschnig and R. M. Mader, Extravasation of Pt-based chemotherapeutics – tissue bioimaging by LA-ICP-MS, *Metallomics*, 2015, **7**, 508–515.
43 M. Svartengren, C. G. Elinder, L. Friberg and B. Lind, Distribution and concentration of cadmium in human kidney, *Environ. Res.*, 1986, **39**, 1–7.
44 C. Kent, *Basics of Toxicology*, John Whiley & Sons, 1998.